Instituto Tecnológico y de Estudios Superiores de Monterrey

Campus Monterrey

School of Engineering and Sciences

Induced Rotation of Ratchets in Passive Environments

A thesis presented by

Yeray Cruz Ruiz

Submitted to the
School of Engineering and Sciences
in partial fulfillment of the requirements for the degree of

Master
In
Nanotechnology

Monterrey, Nuevo León, México, Nov 2025

Instituto Tecnológico y de Estudios Superiores de Monterrey

Campus Monterrey School of Engineering and Sciences

The commitee members, hereby, certify that have read the thesis presented by **Yeray Cruz Ruiz** and that it is fully adequate in scope and quality as a partial requirement for the degree of Master in Nanotechnology.

_____

Antonio Ortiz Ambriz, PhD
Thesis Advisor
School of Engineering Sciences, Tecnológico de Monterrey

_____

Someone, PhD
Sinodal member
Affiliation

_____

Someone, PhD
Sinodal member
Affiliation

_____

Someone, PhD
Sinodal member
Affiliation

_____

Dr. Elisa Virginia Vázquez Lepe
Graduate Studiates Director
School of Engineering and Sciences
Monterrey, Nuevo León, México, May 2025

Declaration of Authorship

I, Yeray Cruz Ruiz (student), declare that this thesis titled, “Induced Rotation of Ratchets in Passive Environments” and the work presented in it are my own. I confirm that:

- This work was done wholly or mainly while in candidature for a research degree at this University.
- Where any part of this thesis has previously been submitted for a degree or any other qualification at this University or any other institution, this has been clearly stated.
- Where I have consulted the published work of others, this is always clearly stated.
- Where I have quoted from the work of others, the source is always given. Apart from such quotations, this thesis is entirely my own work.
- I have acknowledged all main sources of help.
- Where the thesis is based on work done by myself jointly with others, I have made clear exactly what was done by others and what I have contributed myself.

_____

Yeray Cruz Ruiz (Student)
Monterrey, Nuevo León, México, May 2025

Dedication

For those who come after.

Acknowledgements

To my parents for their unwavering support, to my friends for making this journey easier, and especially to Dr. Antonio, who always believed in me and was an incredible mentor.

Induced Rotation of Ratchets in Passive Environments

by

Yeray Cruz Ruiz

Abstract

Swimming at the mesoscale has been a topic of interest for the past two decades because of the complexity of motion at a low Reynolds number, a regime where the viscous forces dominate over the inertial ones. The scallop theorem is a principle that follows these complex ideas and states that a scallop, which has only one degree of freedom, must be unable to have net displacement in this regime due to the lack of time-reversal symmetry of the Navier-Stokes equations. Indifferent to our mathematical understanding, nature was capable of creating biological beings that are able to displace under these circumstances by developing what we call nonreciprocal motion. The esquerichia coli, for example, has a flagellum that rotates in one direction, pushing the fluid backwards and therefore moving the bacteria forwards. Inspired by these ideas, researcher have taken interest in generating motion at those scales. One example are bacterial micromotors, where a dented ratchet is immersed into a bacterial bath where they convert energy from their surroundings into movement. This movement normally follows a ballistic trajectory and in time some of them, will collide into the ratchet transferring their kinetic energy, and therefore making the motor spin thanks to the geometry of the ratchet. Unfortunately, the nutrients they absorb will end and in time the system's medium will need to be replaced, stopping the whole process, therfore being an inneficient process. This is a type of active matter that gets energy from its medium. But, Can we do the same with passive matter?

In this work, we analsze paramagnetic colloids, manipulated by an external precessing magnetic field. The system is confined betwen the z axis and presents periodic boundary conditions in x, and y axis. When multiple particles are present, dipole-dipole interactions arise, leading to either attraction or repulsion depending on their head-to-tail alignment. The particles' internal fields also rotate, dynamically altering their interactions over time. We observe that from 0Hz to 3Hz, the colloids form pairs and start rotating with a shared center of mass, whereas from 3.25 to 7Hz particles have a moment of replsion, creating a neighbor exchange between different pairs, obtaining a ballistic trajectorWe observe that from 0Hz to 3Hz, the colloids form pairs and start rotating with a shared center of mass, whereas from 3.25 to 7Hz particles have a moment of replsion, creating a neighbor exchange between different pairs, obtaining a ballistic trajectory. To investigate whether this motion can perform work, we place a ratchet-like object with different parameters amidst the particles.

List of Figures

List of Tables

Contents

Part I

Introduction

Chapter 1

Introduction

Part II

Background

Chapter 2

Physics at the mesoscale

2.1 Low Renolds number regime

At the mesoscale, where objects such as bacteria and colloidal particles operate, the physical world is governed by a regime in which viscous forces dominate over inertial ones. This regime is characterized by a small Reynolds number (Re), a dimensionless quantity that compares inertial to viscous effects. Therefore, the force applied at that moment will describe the movement or displacement performed, not deppending on any past force, this is a characteristic of an overdamped system. In his seminal lecture, Life at Low Reynolds Number, Purcell highlighted the surprising and often counterintuitive behaviors that emerge in such environments [1]. For instance, time-reversible motion — common at macroscopic scales — is ineffective for propulsion at low Re, necessitating non-reciprocal strategies like flagellar rotation or body undulation. This leads to the scallop theorem, that states that an animal with such degrees of freedom — in a viscous regime — will not have a net displacement.

This whole process can be described by the Navier-Stokes equation without the inertia terms, leaving us without any time deppending terms as shown in 2.1.

$$-\nabla p + \eta \nabla^2 \vec{v} = 0 \tag{2.1}$$

This has been a topic of interest for researchers that are constantly looking for ways of transportation in those environments for specific tasks. Unfortunately this is not the only challenge we face when moving at the microscale.

2.2 Brownian Motion and Thermal Fluctuations

Even though this is a viscous regime, particles are not static. At small length scales, such as those of colloidal particles or bacteria, random thermal fluctuations become a dominant source of motion. This phenomenon, known as *Brownian motion*, was first explained quantitatively by Albert Einstein in 1905. He demonstrated that the irregular paths observed in microscopic particles suspended in fluid result from collisions with the molecules of the surrounding medium [2].

Einstein's work provided one of the first convincing arguments for the molecular nature of matter and led to a mathematical description of how these random movements accumulate over time. Specifically, he derived that the mean squared displacement (MSD) of a particle grows linearly with time:

$$\langle x^2(t) \rangle = 2Dt, \tag{2.2}$$

where D is the diffusion coefficient, a measure of how quickly particles spread out. Einstein further related this coefficient to measurable physical parameters through the expression:

$$D = \frac{k_B T}{6\pi\eta R}, \tag{2.3}$$

where k_B is Boltzmann's constant, T the absolute temperature, η the dynamic viscosity of the fluid, and R the radius of the spherical particle. This relation — often referred to as the *Einstein-Stokes equation* — is foundational in soft matter and colloidal physics.

In the systems considered in this thesis, Brownian motion plays a crucial role in the dynamics of passive colloids and must be accounted for even in the presence of external fields or active agents, such as bacteria.

While Einstein's formulation captures the long-term diffusive behavior of Brownian particles, it does not account for their instantaneous dynamics. To describe how particles move under both viscous damping and random thermal forces, we turn to a stochastic differential equation known as the *Langevin equation*.

2.2.1 Stochastic Representation

The Langevin equation [3] in one dimension, including inertial effects, damping, and thermal noise, can be written as:

$$m\ddot{x} = F - \lambda\dot{x} + \eta(t), \tag{2.4}$$

where m is the particle mass, λ is the damping coefficient, and $\eta(t)$ is a stochastic force representing thermal noise. For simplicity, we write the velocity as $v = \dot{x}$, leading to:

$$m\frac{dv}{dt} = F - \lambda v + \eta(t). \tag{2.5}$$

Discretizing time with a small step dt, we apply the definition of a derivative:

$$m\frac{v(t+dt) - v(t)}{dt} = F - \lambda v(t) + \eta(t). \tag{2.6}$$

The thermal noise term $\eta(t)$ is modeled as a Gaussian white noise process:

$$\eta(t)\, dt = g\, dW, \tag{2.7}$$

where dW is a Wiener process (increment of Brownian motion) such that:

$$\langle dW \rangle = 0\,, \quad \langle dW^2 \rangle = dt. \tag{2.8}$$

Solving for $v(t+dt)$ gives:

$$v(t+dt) = v(t) + \frac{dt}{m}(F - \lambda v(t)) + g\, dW. \tag{2.9}$$

Now, assuming no deterministic force ($F = 0$) — as is the case for free passive particles:

$$v(t+dt) = v(t) - \frac{\lambda dt}{m} v(t) + g\, dW. \tag{2.10}$$

Taking the expectation value (mean) of both sides:

$$\langle v(t+dt) \rangle = \langle v(t) \rangle - \frac{\lambda dt}{m} \langle v(t) \rangle + g \langle dW \rangle. \tag{2.11}$$

Since $\langle dW \rangle = 0$, the last term vanishes:

$$\langle v(t+dt) \rangle = \langle v(t) \rangle \left(1 - \frac{\lambda dt}{m}\right). \tag{2.12}$$

In the limit of small dt, this leads to the differential equation:

$$\frac{d}{dt}\langle v(t) \rangle = -\frac{\lambda}{m} \langle v(t) \rangle, \tag{2.13}$$

whose solution is:

$$\langle v(t) \rangle = \langle v(0) \rangle\, e^{-\lambda t/m}. \tag{2.14}$$

This result shows that the average velocity of a particle in a viscous fluid decays exponentially due to damping. The characteristic timescale $\tau = m/\lambda$ describes how quickly the particle forgets its initial velocity, after which the motion becomes diffusive.

2.2.2 Velocity Statistics and Energy Equipartition

To compute the variance of the velocity, we start again from the Langevin equation in discretized form, without external forces:

$$v(t+dt) = v(t) - \frac{\lambda}{m}v(t)dt + \frac{g}{m}dW. \tag{2.15}$$

Squaring both sides:

$$v(t+dt)^2 = \left[v(t) - \frac{\lambda}{m}v(t)dt + \frac{g}{m}dW\right]^2, \tag{2.16}$$

$$= v(t)^2 + \left(\frac{\lambda}{m}\right)^2 v(t)^2dt^2 + \left(\frac{g}{m}\right)^2 dW^2 - 2\frac{\lambda}{m}v(t)^2dt + 2\frac{g}{m}v(t)dW - 2\frac{\lambda g}{m^2}v(t)dW. \tag{2.17}$$

Now we take the expectation value:

$$\langle v(t+dt)^2\rangle = \langle v(t)^2\rangle + \left(\frac{\lambda}{m}\right)^2 \langle v(t)^2\rangle dt^2 + \left(\frac{g}{m}\right)^2 \langle dW^2\rangle - 2\frac{\lambda}{m}\langle v(t)^2\rangle dt + 2\frac{g}{m}\langle v(t)\rangle\langle dW\rangle - 2\frac{\lambda g}{m^2}\langle v(t)\rangle\langle dW\rangle. \tag{2.18}$$

Using the properties of the Wiener process:

$$\langle dW\rangle = 0, \quad \langle dW^2\rangle = dt.$$

And neglecting second-order small terms (dt^2), we obtain:

$$\langle v(t+dt)^2\rangle = \langle v(t)^2\rangle + \frac{g^2}{m^2}dt - 2\frac{\lambda}{m}\langle v(t)^2\rangle dt. \tag{2.19}$$

Taking the continuous limit:

$$\frac{d}{dt}\langle v(t)^2\rangle = -2\frac{\lambda}{m}\langle v(t)^2\rangle + \frac{g^2}{m^2}. \tag{2.20}$$

This is a linear first-order ODE. Solving it with variation of constants yields:

$$\langle v(t)^2 \rangle = \frac{g^2}{2\lambda m} + De^{-2\lambda t/m}. \tag{2.21}$$

As $t \to \infty$, the exponential term vanishes and we get the stationary value:

$$\langle v(\infty)^2 \rangle = \frac{g^2}{2\lambda m}. \tag{2.22}$$

From the equipartition theorem, we know that the average kinetic energy is:

$$\frac{1}{2} m \langle v^2 \rangle = \frac{1}{2} k_B T.$$

Therefore:

$$\langle v^2 \rangle = \frac{k_B T}{m}. \tag{2.23}$$

Matching this to our stochastic result:

$$\frac{k_B T}{m} = \frac{g^2}{2\lambda m} \quad \Rightarrow \quad g^2 = 2\lambda k_B T, \quad g = \sqrt{2\lambda k_B T}. \tag{2.24}$$

This defines the noise amplitude in terms of temperature, viscosity, and Boltzmann's constant.

2.2.3 Overdamped Dynamics and Diffusion

In the overdamped limit, inertia is negligible, so the Langevin equation becomes:

$$0 = F - \lambda \frac{dx}{dt} + \eta(t). \tag{2.25}$$

Solving for the velocity:

$$\frac{dx}{dt} = \frac{1}{\lambda}(F + \eta(t)). \tag{2.26}$$

For free diffusion ($F = 0$):

$$\frac{dx}{dt} = \frac{1}{\lambda}\eta(t). \tag{2.27}$$

Using stochastic calculus with $\eta(t)dt = gdW$, we write:

$$x(t + dt) = x(t) + \frac{g}{\lambda} dW. \tag{2.28}$$

Mean Position Taking the expectation:

$$\langle x(t+dt)\rangle = \langle x(t)\rangle + \frac{g}{\lambda}\langle dW\rangle = \langle x(t)\rangle. \tag{2.29}$$

So the mean position remains constant in free diffusion.

Mean Square Displacement (MSD) Squaring the position update:

$$x(t+dt)^2 = x(t)^2 + 2\frac{g}{\lambda}x(t)dW + \left(\frac{g}{\lambda}\right)^2 dW^2. \tag{2.30}$$

Taking the expectation:

$$\langle x(t+dt)^2\rangle = \langle x(t)^2\rangle + 2\frac{g}{\lambda}\langle x(t)\rangle\langle dW\rangle + \frac{g^2}{\lambda^2}\langle dW^2\rangle, \tag{2.31}$$

$$= \langle x(t)^2\rangle + \frac{g^2}{\lambda^2}dt. \tag{2.32}$$

In differential form:

$$\frac{d}{dt}\langle x(t)^2\rangle = \frac{g^2}{\lambda^2}. \tag{2.33}$$

Using $g^2 = 2\lambda k_B T$, we substitute:

$$\frac{d}{dt}\langle x(t)^2\rangle = \frac{2k_B T}{\lambda}. \tag{2.34}$$

Integrating gives the mean squared displacement (MSD):

$$\langle x(t)^2\rangle = \frac{2k_B T}{\lambda}t. \tag{2.35}$$

This is the classical diffusion result, where the diffusion coefficient is $D = \frac{k_B T}{\lambda}$, consistent with Einstein's expression.

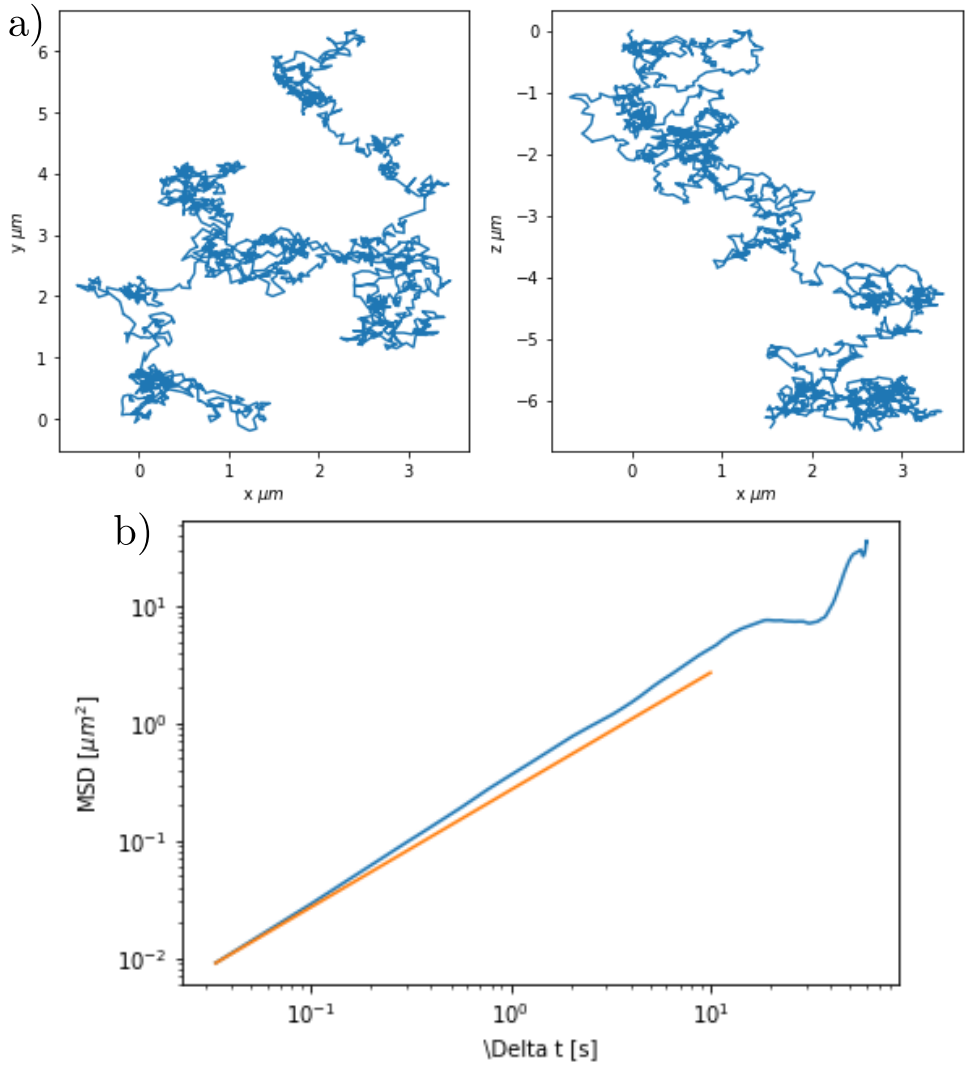

Figure 2.1: A colloidal particle undergoes random, thermally induced displacements in a fluid medium. **Panel a)** shows the trajectory of the particle. **Panel b)** shows the corresponding mean squared displacement (MSD) as a function of time, illustrating the linear relationship predicted by Einstein for diffusive behavior (orange) and the one obtained through a numerical simulation (blue).

Chapter 3

Ratchets and Rectification Mechanisms

3.1 The Feynman-Smoluchowski ratchet

The inherent randomness of Brownian motion naturally leads to the question: can this disorder be transformed into order? In other words, can the random thermal motion of particles be used to produce directed movement or extract work? This question sits at the core of statistical mechanics and was famously explored by Richard Feynman in his lectures on physics, through a thought experiment known as the Feynman ratchet and pawl [4].

The Feynman ratchet consists of a set of vanes connected to a ratchet wheel, immersed in a fluid (Fig. 3.1). The idea is: random collisions from the surrounding molecules could push the vanes, but the pawl only allows rotation in one direction. At first glance, this asymmetric mechanism seems capable of converting random thermal motion into unidirectional rotation, apparently violating the second law of thermodynamics.

However, Feynman's analysis showed that when both the ratchet and the pawl are in thermal equilibrium with the same heat bath, the system cannot produce net work. The pawl itself undergoes thermal fluctuations and can occasionally lift off, allowing the ratchet to move backward. Over time, the forward and backward movements average out, and no net rotation occurs. This result reinforces the principle that thermal fluctuations alone cannot be rectified to perform work without a temperature gradient or an external energy input.

Despite this limitation, the Feynman ratchet introduced a powerful concept: asymmetry combined with non-equilibrium conditions can, in principle, produce directed motion. This idea is foundational in the study of Brownian motors, biomolecular machines, and active matter systems, including the systems explored in this thesis. In such systems, energy is continuously supplied, whether through bacterial metabolism or magnetic field modulation, creating the necessary non-equilibrium environment that allows motion rectification to occur.

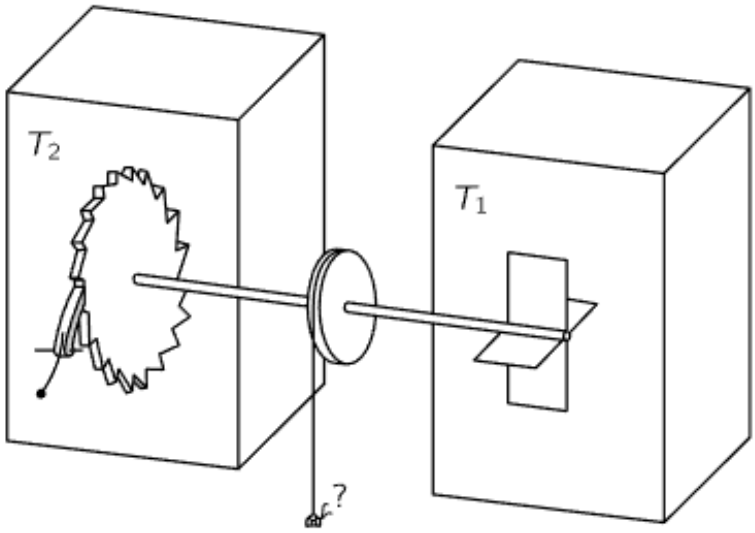

Figure 3.1: Visual representation of the Feynman ratchet. Obtained from [4]

The failure of the Feynman ratchet in thermal equilibrium is intimately connected to another famous thought experiment: Maxwell's demon. Both systems attempt to extract work from thermal fluctuations through selective processes—the ratchet through mechanical asymmetry, and the demon through information gathering.

Maxwell's demon, proposed in 1867, imagines a microscopic being that can sort fast and slow molecules between two chambers, creating a temperature difference without apparent work. Similarly, the pawl in Feynman's ratchet acts as a mechanical "demon," attempting to select only forward fluctuations while blocking backward motion. However, both fail for the same fundamental reason: the cost of selection itself [5, 6].

Brillouin (1951) and later Landauer (1961) showed that Maxwell's demon must expend energy to measure molecular velocities and erase information, with the minimum energy cost being $kT \ln 2$ per bit erased. In the Feynman ratchet, the pawl must "decide" whether to allow motion, and this decision-making process—manifested as thermal fluctuations of the pawl itself—has an entropic cost that exactly cancels any work extracted [7, 8].

This connection reveals a deep principle: rectification requires either an information gradient (knowledge about the system) or an energy gradient (non-equilibrium conditions). As Parrondo and Español (1996) demonstrated, the Feynman ratchet can be viewed as an information engine where the pawl performs measurements on the ratchet's position. When the pawl and ratchet are at the same temperature, the information gained equals the entropy produced, yielding no net work [9].

Table 3.1: Summary of operation of ratchet and pawl. Obtained from [4]

Forward:	Needs energy	$\epsilon + L\theta$ from vane.	$\therefore$ Rate = $\frac{1}{\tau} e^{-(L\theta+\epsilon)/kT_1}$
	Takes from vane	$L\theta + \epsilon$	
	Does work	$L\theta$	
	Gives to ratchet	ϵ	
Backward:	Needs energy	ϵ for pawl.	$\therefore$ Rate = $\frac{1}{\tau} e^{-\epsilon/kT_2}$
	Takes from ratchet	ϵ	
	Releases work	$L\theta$	
	Gives to vane	$L\theta + \epsilon$	

If system is reversible, rates are equal, hence

$$\frac{\epsilon + L\theta}{T_1} = \frac{\epsilon}{T_2}.$$

$$\frac{\text{Heat to ratchet}}{\text{Heat from vane}} = \frac{\epsilon}{L\theta + \epsilon}. \quad \text{Hence} \quad \frac{Q_2}{Q_1} = \frac{T_2}{T_1}.$$

3.2 Brownian ratchets

While Feynman's ratchet fails due to thermal equilibrium, rectified motion becomes possible when detailed balance is broken through external driving. Magnasco (1993) demonstrated this principle through the "rocking ratchet" mechanism [10]. In his model, a Brownian particle moves in an asymmetric periodic potential—essentially a sawtooth-shaped energy landscape with gentle slopes in one direction and steep walls in the other. The crucial innovation was applying an oscillating force $F(t) = A\cos(\omega t)$ that rocks the potential back and forth. Although this force has zero time average—pushing equally left and right—the combination with the spatial asymmetry produces net directional motion. When the force tilts the potential forward, particles easily climb the gentle slopes and can overcome barriers. When tilted backward, particles encounter steep walls and remain trapped. This asymmetric response to symmetric driving breaks the forward-backward symmetry of thermal diffusion.

This mechanism differs fundamentally from Feynman's original ratchet: rather than attempting to rectify equilibrium fluctuations (which violates the second law), the rocking ratchet con-

tinuously injects energy through the oscillating force. The time-dependent driving maintains the system far from equilibrium, enabling the spatial asymmetry to generate directed transport. This principle—that asymmetry plus non-equilibrium driving yields rectification—underlies numerous biological processes and provides the theoretical foundation for the magnetically-driven ratchets explored in this thesis.

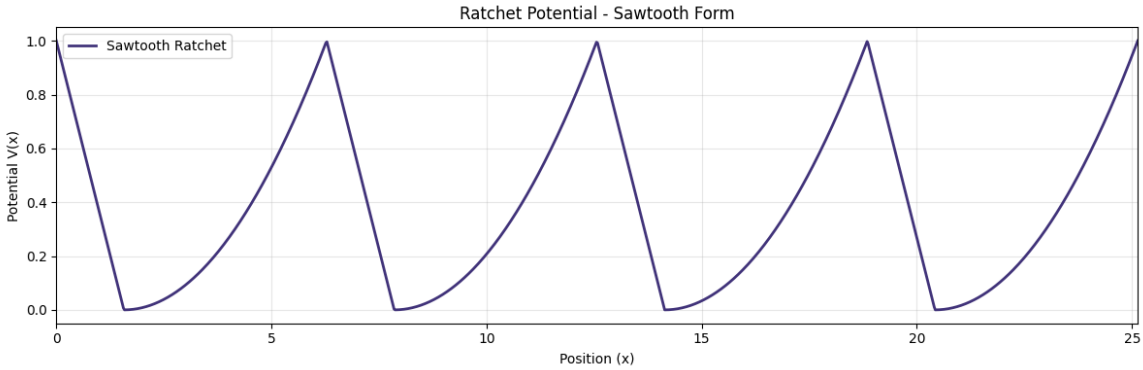

Figure 3.2: Example of a commonly used ratchet potential.

Following Magnasco's rocking ratchet where an oscillating force drives particles in a static potential, Ajdari et al. (1994) analyzed rectification in periodic structures with either spatial or temporal asymmetry [11]. Using a sawtooth potential with asymmetric slopes (steep of height ϵ/a and gentle of ϵ/b), they identified distinct transport regimes as a function of the AC force amplitude γ.

For small forces $\gamma < \epsilon/a$, particles remain trapped. In the intermediate regime $\epsilon/a < \gamma < \epsilon/b$, rectification occurs as particles can climb the gentle slope but not the steep one, yielding either integer velocities $V = n$ when particles fully relax between cycles, or rational velocities $V = n - 1/(m + 1)$ when incomplete relaxation creates a periodic pattern over multiple cycles.

This concept was later demonstrated experimentally by Faucheux et al. (1995), who created an "optical thermal ratchet" using focused laser beams [12]. To generate a circular trap without introducing external forces, they passed the laser through a plate to create circular polarization, maintaining constant laser intensity along the circular path. By rotating the laser frequency fast enough, particles could not experience any directed force from the beam itself, allowing them to move freely, then modulated the beam intensity to create an asymmetric potential mimicking a ratchet shape, as shown in Figure 3.3. They observed that particles localized in potential minima when the modulation was turned on, while for sufficiently long periods, particles moved either backward or forward with equal probability.

A different approach was developed by Lee et al. (2004), who employed holographic optical

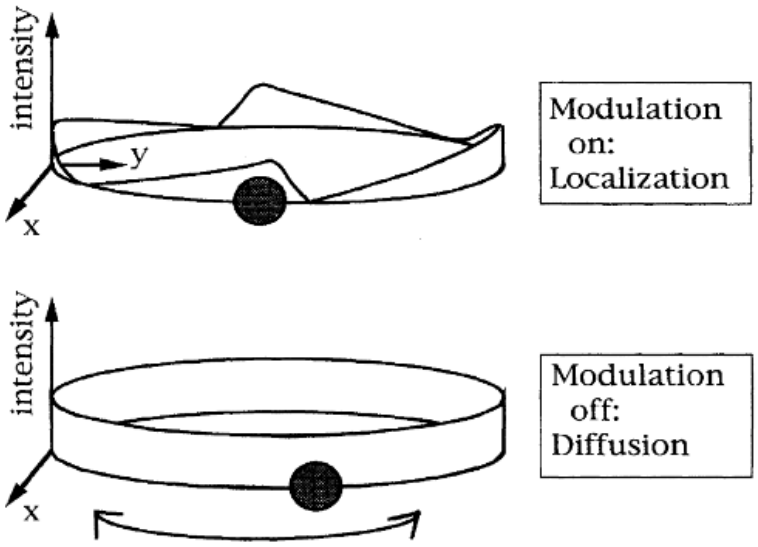

Figure 3.3: When the modulation is on, the beam intensity follows the shape of a ratchet potential with 4 periods per cycle. When the modulation is off, the intensity remains constant, allowing particles to diffuse freely. Obtained from [12].

trapping with a symmetric potential [13]. Their system consisted of discrete optical tweezers functioning as potential wells. Between each state, particles are released and free to diffuse, nevertheless they can rapidly jump between adjacent traps. Using this methodology, they achieved net particle displacement in one direction, as illustrated in Figure 3.4. Remarkably, when they reversed the direction of well displacement, particles followed the trap movement in the opposite direction. Due to this predictable response to trap motion, they named this system a "deterministic thermal ratchet."

Lebedev et al. (2009) modified this approach by using three linearly polarized beams acting only in the xy-plane, as shown in Figure 3.5 [14]. They applied forces to particles by phase-modulating two of the three lasers, which shifts the entire optical lattice. The modulation was generated using RF generators to produce potentials V_x and V_y. The sum $V_x + V_y$ served as the input signal for beam 2, while the difference $V_x - V_y$ was used for beam 3, creating the rocking forces. They studied this system using ultracold rubidium atoms as test particles. To track the atomic positions, they employed a CCD camera to determine the center of mass of the atomic cloud.

In their first experiment, they applied a biharmonic drive along only one axis. As expected, the system reduced to a one-dimensional harmonic ratchet, and they observed directed particle motion along the axis of the applied biharmonic force. In subsequent experiments, they applied

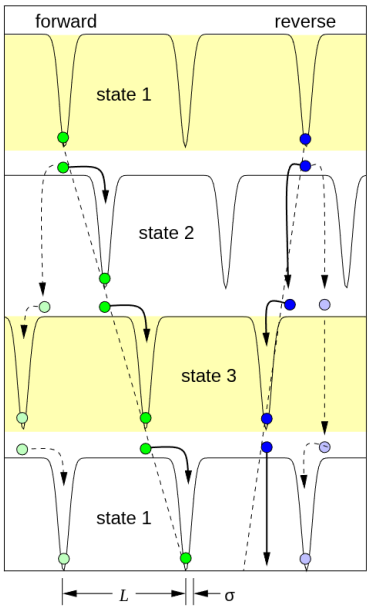

Figure 3.4: Discrete pattern of optical traps with displacement in one directio, minimum width of σ and a maximum width of L. Obtained from [13]

harmonic drives along both axes, with one frequency being twice the other. Their results showed that particles experienced directed motion along the axis with the faster harmonic, while motion along the other axis remained diffusive. In their final experiment, they applied biharmonic drives simultaneously along both axes to investigate whether directed transport could be achieved in two dimensions. By varying the relative weights of the forces along each axis, they demonstrated that it was possible to control the atomic displacement and direct atoms to specific target positions as shown in Figure 3.5 a).

Following the same lattice-based approach, Arzola et al. (2017) successfully recreated all five two-dimensional Bravais lattices using computer-generated holographic optical micromanipulation [15]. Their potential consisted of Gaussian wells distributed along a primary lattice, combined with a shifted replica of the same lattice with a reduced depth factor, Q, compared to the original. The asymmetry of the resulting potential depended directly on both the depth factor Q and the displacement between the original and replica lattices. They implemented the rocking mechanism by moving the particle cell along one axis.

The researchers performed three main experiments to validate their results, each with three different diffusion parameters (including no diffusion as one condition), calculating the current in the x and y axes with respect to the amplitude of movement. In the first experiment, they set the asymmetry parallel to the rocking force. They observed that since the wells were aligned with

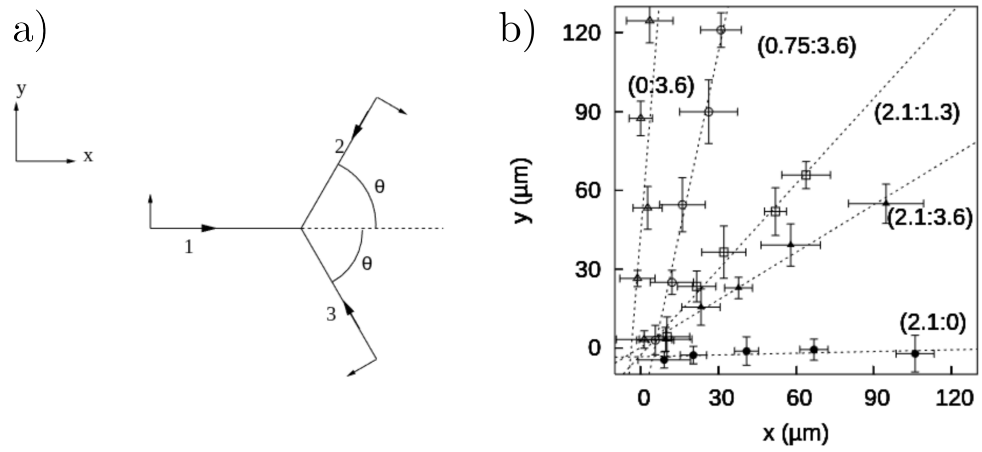

Figure 3.5: Panel a) Lattice beam configuration in the xy plane. $\theta = 60°$. **Panel b)** Position of the atomic cloud center of mass at different instants and forces when applying biharmonic at ehe same time in xy-plane. Obtained from [14].

the particle movement, particles tended to move in the direction of the force, traveling from well to well, while experiencing no movement in the perpendicular direction. Current was present along the entire amplitude range.

The second experiment positioned the asymmetry perpendicular to the rocking force direction, yielding interesting results. Similar to the first experiment, current appeared along only one axis (the asymmetry axis), but the current behaved like a Gaussian bell curve. When the rocking movement amplitude approached the asymmetry lattice spacing, particles only moved back and forth between two wells in the x direction, experiencing no current in the y axis.

For the final experiment, they examined how the system behaved under a combination of both previous configurations. They created an oblique lattice with the asymmetry aligned with the rocking force direction, producing an oblique particle current. The results were essentially a combination of the two previous experiments: at certain amplitudes, current appeared in both axes, but as amplitude increased, the y-axis current decreased while the x-axis current increased. The results for each experiment can be seen in Figure 3.6.

Feynman demonstrated that a purely thermal Brownian ratchet cannot generate directed motion due to the second law of thermodynamics. However, introducing specific conditions to break symmetry has proven ideal for bypassing these limitations.

One successful approach to achieving this symmetry breaking involves rocking ratchets, where an external periodic drive is applied to an asymmetric potential. Previous experiments have demonstrated the potential of optics to create such asymmetries with high precision and

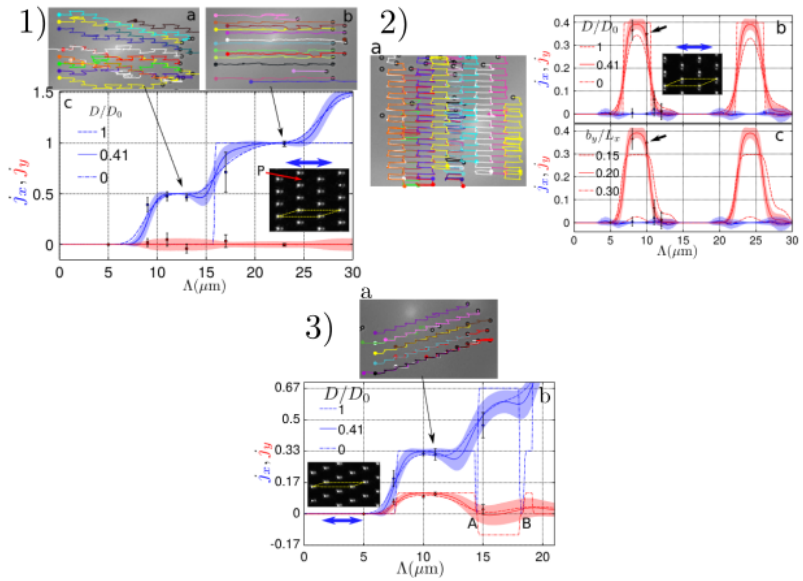

Figure 3.6: Panel 1) Experimental trajectories for assymetry parallel to rocking movement with a) rocking amplitud of 13 μm and b) 23 μm.c) Graphs of simulations showing the current for each axis. **Panel 2)** Experimental trajectories for assymetry perpendicular to rocking movement with a) rocking amplitud of 10 μm. b) and c) Shows the current for each axis with different lattice parameters. **Panel 3)** Experimental trajectories for oblique lattice with assymetry perpendicular to the rocking movement with a) rocking amplitud of 11μm. b) Current for each axis. Obtained from [15].

control. While obtaining directed motion at the microscale remains challenging, by applying these symmetry-breaking parameters it becomes possible not only to overcome thermal noise but to harness it for directional transport. Unfortunately, as shown in previous works, implementing these systems often requires specific and sophisticated experimental setups. Interestingly, nature has already developed an alternative solution by creating matter capable of self-propulsion, known as active matter, which achieves directed motion through entirely different mechanisms.

Chapter 4

Active Matter Systems

4.1 Fundamentals of Active Matter

The definition of active matter is not always the same across the literature. Some authors describe it in a broad way, emphasizing that the key element is the continuous intake and dissipation of energy by each unit, which allows them to remain out of equilibrium and sustain motion or internal stresses. Reviews often highlight internally driven systems—such as cytoskeletal extracts, swimming microorganisms, or synthetic colloids—as the most representative examples of active matter [16–18].

Other authors focus more specifically on self-propulsion at the particle level as the defining feature. This perspective is useful for distinguishing active systems from those whose dynamics are mainly caused by externally imposed forces. For example, in vibrated granular monolayers, asymmetric grains can display self-propelled trajectories and flock-like patterns and are sometimes described as active. In contrast, symmetric grains that only move in a directed way because of an asymmetric boundary, such as a sawtooth channel, are better classified as externally driven rather than active [19–21].

There is also a difference when considering individual vs. collective behavior. Some colloids appear passive when studied alone, but when interactions are taken into account, they can exhibit genuinely non-equilibrium collective phenomena. Examples include motility-induced phase separation (MIPS), defect-mediated flows in active nematics, and other emergent patterns normally linked with active matter. For this reason, several reviews describe active matter not only in terms of single-particle propulsion but also in terms of its collective stresses and patterns [22, 23].

Simple theoretical models have played a crucial role in understanding active matter. One of the best-known examples is the Vicsek model, which shows how local alignment rules together with noise can lead to large-scale collective motion from basic self-driven units [24, 25]. At the

level of single particles, the Active Brownian Particle model is a common way to study colloidal swimmers. In this model, motion is explained by a constant propulsion force, combined with random changes in orientation resulting from rotational diffusion [26, 27].

More recent works point out that definitions have evolved over time and suggest clarifying criteria such as whether the drive is internal or external, whether the system is dry or wet (momentum non-conserving or conserving), and whether the energy input acts at the particle level. Some surveys even propose that researchers explicitly state their working definition depending on the context of their problem [28, 29].

Working definition. In this thesis, we define active matter as:

> systems composed of units that continuously draw energy at the particle scale and convert it into mechanical work, generating persistent stresses or self-propulsion, and sustaining non-equilibrium collective dynamics.

This definition includes both biological and synthetic systems (such as bacteria, cytoskeletal extracts, and Janus colloids) but excludes setups where directed motion arises only from externally imposed vibrations or asymmetric boundaries without particle-level energy input—for example, symmetric grains transported by a sawtooth channel [30, 31].

We will first present some macroscopic examples that show universal principles of self-organization, and then move to the microscopic cases most relevant to this work—active colloids, run-and-tumble swimmers, and active nematics—where thermal noise and low-Reynolds-number hydrodynamics play a dominant role.

4.2 Macroscopic Agents

Examples of active matter can be observed at plain sight in the macroscopic world. A flock of birds, for instance, is considered active matter because each bird is capable of self-propulsion. Unlike microscopic systems, they are not significantly affected by the thermal noise of their medium—in this case, air. A computational study by Reynolds (1987) modeled flocking behavior in birds by treating each individual as an autonomous agent whose trajectory was influenced by its local environment and neighboring individuals [32].

Reynolds introduced three fundamental rules governing flocking behavior: separation (collision avoidance), alignment (velocity matching with neighbors), and cohesion (attraction toward the average position of neighbors). This work laid the foundation for understanding how simple local interactions can give rise to complex patterns of collective motion.

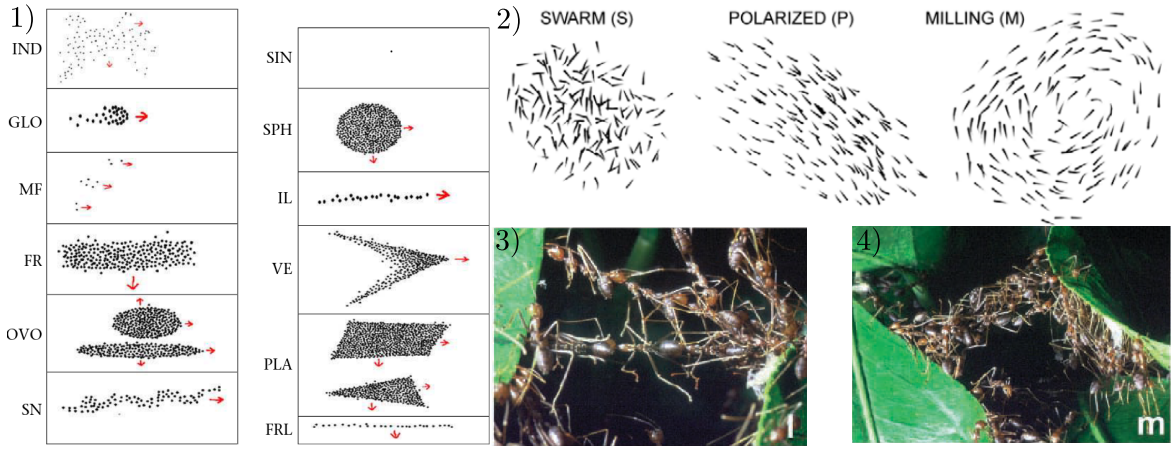

Figure 4.1: Panel 1) Example of different formation of birds deppending predation risk, obtained from [35]. **Panel 2)** Different formation of schooling fish, obtained from [40]. **Panel 3) - 4)** Aggregation of ants forming a bridge, obtained from [41].

Over time, further developments in the study of group dynamics have incorporated methods such as dynamical maximum entropy to predict the alignment of ordered groups [33]. Following a maximum entropy approach, network reshuffling was later studied [34]. These behaviors, however, can change due to external factors, such as predation risk, which influences the formation and density of flocks [35]. In addition, individual characteristics can also affect collective behavior [36].

There are also self-organized groups of smaller flying animals whose collective behavior is even more complex than that of larger species. For example, bees are capable of dividing labor as a result of social interactions among individuals [37]. Remaining within the field of insects but shifting to a solid medium, ants exhibit similar patterns of labor division. Their organization can transition between ordered and disordered states depending on colony size. The disordered state typically occurs when the number of foraging ants is small, due to the infrequent discovery of food [38]. However, even when the colony is large enough to sustain a greater number of foragers, problems can still arise. In particular, some ants may remain stationary, occupying tunnels and thereby reducing the overall flow rate [39].

Another characteristic that arises from self-organization in ants—one not possessed by all animals—is their ability to self-assemble to perform specific tasks. Examples include the formation of rafts, bridges, or columns, where each individual uses its legs or jaws to grasp another and remains in place until the collective goal is achieved. Naturally, certain factors influence these self-assemblages, one of the most significant being colony size [41]. Interesntingly, these structures posses some viscoelastic properties, when applied a certain stress, they tend to return

to their original place, resulting in an elastic behavior, at the same time they adapt a viscous behavior due to objects being able to sink in the aggreagation, the same way they would do in a viscous fluid [42]. This opens the posibility for ants to be used as smart materials.

There are also animals that form groups while inhabiting more complex environments, such as water. Regardless of the medium, different species often display similar behaviors and dependencies. For example, the dynamics of schooling fish can be predicted, typically resulting in three main configurations, with variations depending on group size [40, 43, 44].

These are just few examples of large animal groups that, interestingly, share common characteristics of self-organization. This process begins at the level of the individual but emerges as a collective, temporary order through direct or indirect interactions among organisms, ultimately allowing them to achieve a common goal [45].

The study of macroscopic agents reveals that self-organization is not limited to large animal groups. At smaller scales, microscopic agents such as bacteria, colloidal particles, and artificial swimmers also exhibit analogous self-organized behaviors, although these are driven by different physical principles, including thermal noise and low-Reynolds-number hydrodynamics.

4.3 Microscopic agents

As discussed in the previous section, the term active matter is not limited to microscopic systems but also applies to animal groups. However, the focus of this thesis will be on the former.

We have already defined how a passive brownian particle acts, therefore let us review the key difference of active and passive ones. Passive particles undergo mere diffusion motion, whereas active follows stochastic differential equations accordnig to [46]:

$$\frac{d}{dt}x(t) = v\cos\varphi(t) + \sqrt{2D_T}W_x, \tag{4.1}$$

$$\frac{d}{dt}y(t) = v\sin\varphi(t) + \sqrt{2D_T}W_y, \tag{4.2}$$

where W_x, and W_y represent their corresponding Wiener process, and v is the mean velocity. As stated before, if

$$\lim_{v\to 0} v\cos\varphi(t) + \sqrt{2D_T}W_x, \tag{4.3}$$

then the motion is merely diffusive and the particle is characterized as passive brownian particle.

However, they also exhibit some randomness; it is rare for them to move exactly in a straight line, and this is where chirality comes into play. There are three different forms of asymmetry:

rotational, reflexional, and a combination of the two. If a particle does not meet any of the three criteria, then the particle is not symmetric in any aspect. Chirality is actually the name for a non-reflexive-symmetric particle, as exemplified by our hands, from which the actual word originates [47].

Therefore adding an important third term for the rotational diffusion given by:

$$\frac{d}{dt}\varphi = \sqrt{2D_R}W_\varphi. \tag{4.4}$$

Despite this limitations, researchers have been developing new methods to achieve self-propulsion that mimic natural processes. In the following subsections, we will introduce a few examples of different systems that have been created, as well as organic ones.

4.3.1 Artificial Systems

As discussed in Section 4.1, the definition encompasses various mechanisms of self-propulsion, and the list and discoveries are extensive.

Take, for example, *PDMS platelets coated with Pt* by Ismagilov et al. (2002), it appears to be the first realization of this method. The motion itself is not performed by the particle, but by the layer of platinum (catalyst). This is a chemical reaction where the components move by the releasing of bubbles produced when a liquid (hydrogen peroxide) breaks down with the help of a catalyst [48]. If we examine the definition of a catalyst, this one does not seem to be affected by the reaction; therefore, the movement would occur indefinitely. In fact, under the experiment's conditions, they achieved an uninterrupted motion of approximately 2 hours.

In the movement of the particles, they saw that they do not move in a straight line but rather in a circular manner, which is due to the chirality. They observed this behavior in all the particles; however, it was not completely identical.

This experiment opened up the possibility of different setups; the previous one, where plain plates were used, raises a question: Does this behavior depend on the shape of the particle? Paxton et al. (2004) did a similar experiment with a slightly different setup, utilizing rods with a diameter of 370 nms, with 2 stripes of platinum and gold, each one of 1 μm long in the direction of the long axis. Recalling the previous experiment, platinum is a catalyst for hydrogen peroxide; however, the twist here is that gold is not [49]. Although the setup was similar, using the same chemicals, the results differed. They observed that the rods had a tendency to move along their elongated section, particularly where the platinum was located, yielding a different result from the previous experiment, where the particle moved in the opposite direction to the platinum.

Not so much time later, Dreyfus et al. (2005) claimed that at that point, there was no artificial swimmer that had a *controlled swimming motion* [50]. They combined organic and artificial ele-

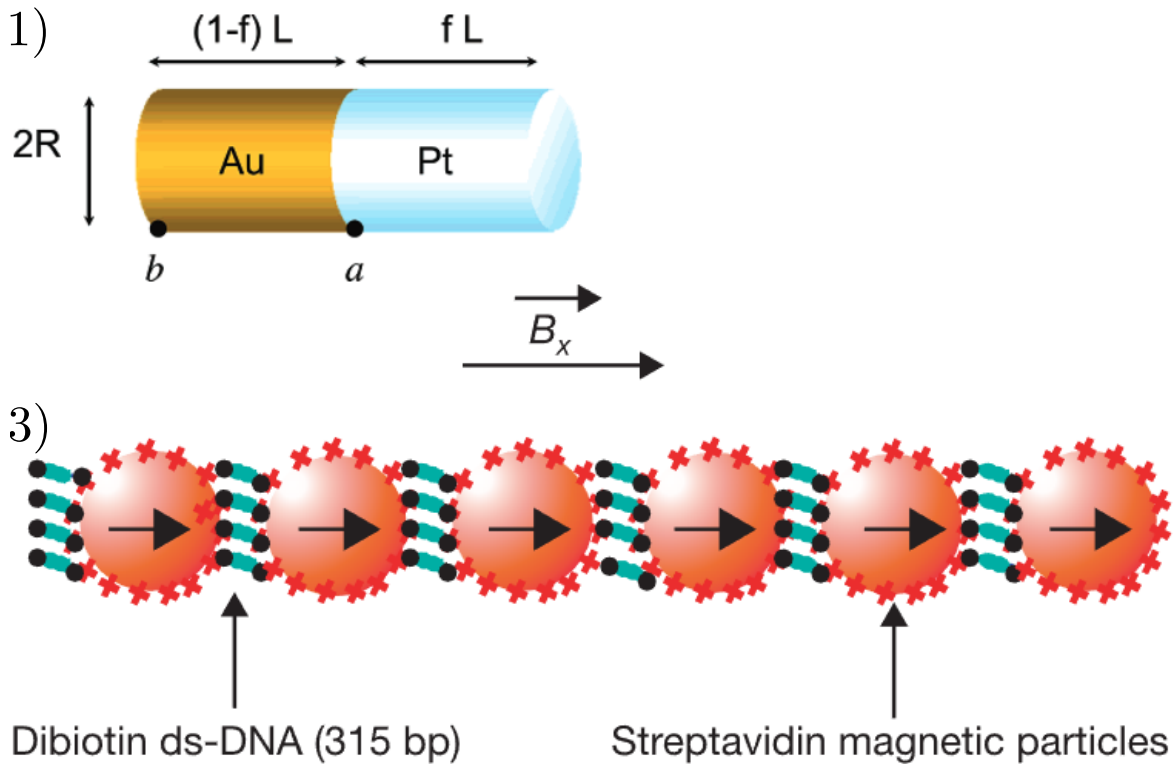

Figure 4.2: **Panel 1)** shows the configuration of nanorods of Gold (Au) and Platinum (Pt), obtained from [49]. **3** shows a chain of red blood cells linked with superparamagnetic filaments, obtained from [50].

ments; they used superparamagnetic filaments that respond to a magnetic field. These filaments are attached to a red blood cell, joining multiple to obtain a chain. To control the behavior of the filaments, they used two magnetic fields: a constant field parallel to the filament and a sinusoidal field perpendicular to the filament. With this approach, they were not only able to control the direction but also the speed by adjusting the frequency of the sinusoidal field, and the direction towards the parallel field.

However Howse et al. (2007) established the experimental basis for active Brownian particle dynamics by studying self-motile colloidal particles that use chemical reactions catalyzed on their surface to achieve autonomous propulsion. They demonstrated that at short times, these particles exhibit substantial directed motion with velocity dependent on fuel concentration, while at longer times, the motion transitions to a random walk with enhanced diffusion coefficients. This work provided a comprehensive experimental validation of the theoretical active Brownian particle model and established the standard mathematical framework for describing such systems through stochastic differential equations [51, 52]. These were done by coating polystyrene sh-

peres with a layer of platinum, the same process as the plates and the nanorods, which will be the responsible of the propulsion method, nontheless, this in not inherently of the particle's shape, there have been assymetric artificial particles with an L shape that undergoes the same behavior [53].

Figure 4.3 helps visualize how the motion varies according to their velocity. When the average velocity is zero, the linear behavior of the MSD represents a diffusive behavior, whereas when it is different it is considered to be ballistic.

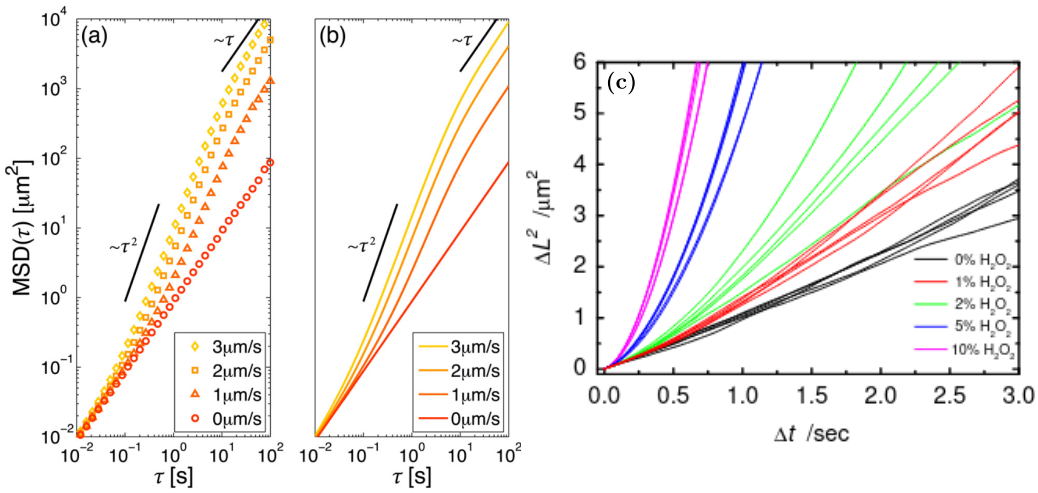

Figure 4.3: MSD for brownian particles with different velocites. **Panel a)** shows the result from simulations. **Panel b)** shows the theoretical calculation, obtained from [46]. **Panel c)** MSD for different velocities of polystyren spheres, obtained from [51].

4.3.2 Organic Systems

This open a new term that appears active brownian particles have, it is called chirality, which is the tendency to move in a circular path just as described by the random walk, however, this movement was only studied in a 2-dimensions confined space. In a research by Corkidi et al. (2008) spermatozoa behavior was studied in a 3-dimensions space mimicking their real environment in searh for eggs, what they found was a helical trajectory, shown in Figure 4.4, being a pretty similar response, and obtaining a non-space dependant behavior [54].

It seems we cannot avoid randomness even for active particles, in a regime where viscous forces are predominant, a little symmetry breaking noise that perturbs the direction of the particle can make the origin of a random walk, but nature, as always, has evolved elegant solutions to this challenge through various biological mechanisms. A prime example is E. coli, which

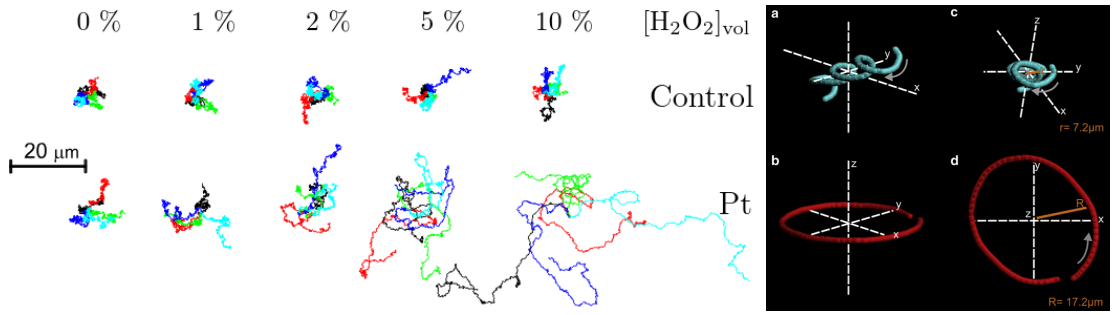

Figure 4.4: Trajectories of polystyren platinum layered sphere particles for different peroxide consentrations, obtained from [51].Trajectory of the spermatozoa for **a,c** free space, and **b, d** confined 2-dimension space. Obtained from [54].

employs helical flagella that can rotate both clockwise and counterclockwise, generating two distinct types of motion that researchers have termed ”run”—swimming in a straight line—and ”tumble”—rotation in a random direction. This behavior also depends on the medium’s viscosity and random fluctuations [55]. The way E. coli achieves a ”run” state is due to their flagella which has two different motions for its power and recovery strokes, simulating those of a human breast strokes, although a tumble state is unavoidable, it is a great opportunity to harness the directed motion of the particle and see if it is possible to obtain work of it.

4.4 Interaction with non-homogeneous environments

All this properties considered an ideal environment, where no obstacles are present. Active particles in real environments encounter surfaces, confinement, and flow fields that dramatically alter their behavior. A striking example is the work by Hill et al. (2007), who demonstrated that E. coli swimming near surfaces in shear flow exhibit sophisticated rheotaxis - the ability to sense flow gradients and actively swim upstream through hydrodynamic surface interactions [56].

4.5 Active motors

Chapter 5

Magnetically Driven Colloidal Systems

5.1 Magnetic Colloids under static fields

5.2 Dynamic Magnetic Actuation

Active matter requires a continuous source of energy to avoid falling under the category of Brownian particles. However, for complex challenges—such as transportation—these systems can tend to be inefficient due to their energy depletion.

Fortunately, Ostinato et al. (2024) Dimer formation, exchange dynamics

Emergent currents withouth self-propulsion

In the study of motion at small scales, materials are often categorized as either active or passive. This distinction is based on whether the constituents are capable of autonomously converting energy into motion.

This thesis focuses on such externally driven passive systems, particularly on paramagnetic colloids subjected to dynamic magnetic fields. These systems provide a controlled platform to study non-equilibrium transport and rectified motion, drawing inspiration from active matter while remaining fundamentally passive in nature.

Bibliography

[1] Edward M Purcell. Life at low reynolds number. In *Physics and our world: reissue of the proceedings of a symposium in honor of Victor F Weisskopf*, pages 47–67. World Scientific, 2014.

[2] Albert Einstein. On the theory of the brownian movement. *Ann. Phys*, 19(4):371–381, 1906.

[3] George E Uhlenbeck and Leonard S Ornstein. On the theory of the brownian motion. *Physical review*, 36(5):823, 1930.

[4] Richard Phillips Feynman. The feynman lectures on physics. *(No Title)*, 1:46, 1963.

[5] James Clerk Maxwell. *Theory of Heat*. Longmans, Green and Co., London, 1871. The demon first appears in Chapter 22.

[6] James Clerk Maxwell. Letter to peter guthrie tait, December 11 1867. First mention of the demon concept.

[7] Léon Brillouin. Maxwell's demon cannot operate: Information and entropy. i. *Journal of Applied Physics*, 22(3):334–337, 1951.

[8] Rolf Landauer. Irreversibility and heat generation in the computing process. *IBM Journal of Research and Development*, 5(3):183–191, 1961.

[9] Juan MR Parrondo and Pep Español. Criticism of feynman's analysis of the ratchet as an engine. *American Journal of Physics*, 64(9):1125–1129, 1996.

[10] Marcelo O Magnasco. Forced thermal ratchets. *Physical Review Letters*, 71(10):1477, 1993.

[11] Armand Ajdari, David Mukamel, Luca Peliti, and Jacques Prost. Rectified motion induced by ac forces in periodic structures. *Journal de Physique I*, 4(10):1551–1561, 1994.

[12] Luc P Faucheux, LS Bourdieu, PD Kaplan, and Albert J Libchaber. Optical thermal ratchet. *Physical review letters*, 74(9):1504, 1995.

[13] Sang-Hyuk Lee, Kosta Ladavac, Marco Polin, and David G Grier. Observation of flux reversal in a symmetric optical thermal ratchet. *Physical review letters*, 94(11):110601, 2005.

[14] V Lebedev and F Renzoni. Two-dimensional rocking ratchet for cold atoms. *Physical Review A—Atomic, Molecular, and Optical Physics*, 80(2):023422, 2009.

[15] Alejandro V Arzola, Mario Villasante-Barahona, Karen Volke-Sepúlveda, Petr Jákl, and Pavel Zemánek. Omnidirectional transport in fully reconfigurable two dimensional optical ratchets. *Physical review letters*, 118(13):138002, 2017.

[16] Sriram Ramaswamy. The mechanics and statistics of active matter. *Annu. Rev. Condens. Matter Phys.*, 1(1):323–345, 2010.

[17] M Cristina Marchetti, Jean-François Joanny, Sriram Ramaswamy, Tanniemola B Liverpool, Jacques Prost, Madan Rao, and R Aditi Simha. Hydrodynamics of soft active matter. *Reviews of modern physics*, 85(3):1143–1189, 2013.

[18] Clemens Bechinger, Roberto Di Leonardo, Hartmut Löwen, Charles Reichhardt, Giorgio Volpe, and Giovanni Volpe. Active particles in complex and crowded environments. *Reviews of modern physics*, 88(4):045006, 2016.

[19] Julien Deseigne, Olivier Dauchot, and Hugues Chaté. Collective motion of vibrated polar disks. *Physical review letters*, 105(9):098001, 2010.

[20] Shahin Mobarakabadi, Ehsan Nedaaee Oskoee, Matthias Schröter, and Mehdi Habibi. Granular transport in a horizontally vibrated sawtooth channel. *Physical Review E—Statistical, Nonlinear, and Soft Matter Physics*, 88(4):042201, 2013.

[21] Alberto Fernandez-Nieves and Ramon Planet. Active and externally driven granular matter, 2022.

[22] Michael E Cates and Julien Tailleur. Motility-induced phase separation. *Annu. Rev. Condens. Matter Phys.*, 6(1):219–244, 2015.

[23] Amin Doostmohammadi, Jordi Ignés-Mullol, Julia M Yeomans, and Francesc Sagués. Active nematics. *Nature communications*, 9(1):3246, 2018.

[24] Tamás Vicsek, András Czirók, Eshel Ben-Jacob, Inon Cohen, and Ofer Shochet. Novel type of phase transition in a system of self-driven particles. *Physical review letters*, 75(6): 1226, 1995.

[25] Hugues Chaté, Francesco Ginelli, Guillaume Grégoire, and Franck Raynaud. Collective motion of self-propelled particles interacting without cohesion. *Physical Review E—Statistical, Nonlinear, and Soft Matter Physics*, 77(4):046113, 2008.

[26] Pawel Romanczuk, Markus Bär, Werner Ebeling, Benjamin Lindner, and Lutz Schimansky-Geier. Active brownian particles: From individual to collective stochastic dynamics. *The European Physical Journal Special Topics*, 202(1):1–162, 2012.

[27] Jens Elgeti, Roland G Winkler, and Gerhard Gompper. Physics of microswimmers—single particle motion and collective behavior: a review. *Reports on progress in physics*, 78(5): 056601, 2015.

[28] Gerhard Gompper, Roland G Winkler, Thomas Speck, Alexandre Solon, Cesare Nardini, Fernando Peruani, Hartmut Löwen, Ramin Golestanian, U Benjamin Kaupp, Luis Alvarez, et al. The 2020 motile active matter roadmap. *Journal of Physics: Condensed Matter*, 32 (19):193001, 2020.

[29] Gerhard Gompper, Howard A Stone, Christina Kurzthaler, David Saintillan, Fernado Peruani, Dmitry A Fedosov, Thorsten Auth, Cecile Cottin-Bizonne, Christophe Ybert, Eric Clément, et al. The 2025 motile active matter roadmap. *Journal of Physics: Condensed Matter*, 37(14):143501, 2025.

[30] Peter Reimann. Brownian motors: noisy transport far from equilibrium. *Physics reports*, 361(2-4):57–265, 2002.

[31] Peter Hänggi and Fabio Marchesoni. Artificial brownian motors: Controlling transport on the nanoscale. *Reviews of Modern Physics*, 81(1):387–442, 2009.

[32] Craig W Reynolds. Flocks, herds and schools: A distributed behavioral model. In *Proceedings of the 14th annual conference on Computer graphics and interactive techniques*, pages 25–34, 1987.

[33] Andrea Cavagna, Irene Giardina, Francesco Ginelli, Thierry Mora, Duccio Piovani, Raffaele Tavarone, and Aleksandra M Walczak. Dynamical maximum entropy approach to flocking. *Physical Review E*, 89(4):042707, 2014.

[34] Thierry Mora, Aleksandra M Walczak, Lorenzo Del Castello, Francesco Ginelli, Stefania Melillo, Leonardo Parisi, Massimiliano Viale, Andrea Cavagna, and Irene Giardina. Questioning the activity of active matter in natural flocks of birds. *arXiv preprint arXiv:1511.01958*.

[35] Claudio Carere, Simona Montanino, Flavia Moreschini, Francesca Zoratto, Flavia Chiarotti, Daniela Santucci, and Enrico Alleva. Aerial flocking patterns of wintering starlings, sturnus vulgaris, under different predation risk. *Animal behaviour*, 77(1):101–107, 2009.

[36] Iain D Couzin, Jens Krause, Richard James, Graeme D Ruxton, and Nigel R Franks. Collective memory and spatial sorting in animal groups. *Journal of theoretical biology*, 218 (1):1–11, 2002.

[37] Raphaël Jeanson, Penelope F Kukuk, and Jennifer H Fewell. Emergence of division of labour in halictine bees: contributions of social interactions and behavioural variance. *Animal behaviour*, 70(5):1183–1193, 2005.

[38] Madeleine Beekman, David JT Sumpter, and Francis LW Ratnieks. Phase transition between disordered and ordered foraging in pharaoh's ants. *Proceedings of the National Academy of Sciences*, 98(17):9703–9706, 2001.

[39] J Aguilar, D Monaenkova, V Linevich, W Savoie, B Dutta, H-S Kuan, MD Betterton, MAD Goodisman, and DI Goldman. Collective clog control: Optimizing traffic flow in confined biological and robophysical excavation. *Science*, 361(6403):672–677, 2018.

[40] Kolbjørn Tunstrøm, Yael Katz, Christos C Ioannou, Cristián Huepe, Matthew J Lutz, and Iain D Couzin. Collective states, multistability and transitional behavior in schooling fish. *PLoS computational biology*, 9(2):e1002915, 2013.

[41] Carl Anderson, Guy Theraulaz, and J-L Deneubourg. Self-assemblages in insect societies. *Insectes sociaux*, 49(2):99–110, 2002.

[42] Michael Tennenbaum, Zhongyang Liu, David Hu, and Alberto Fernandez-Nieves. Mechanics of fire ant aggregations. *Nature materials*, 15(1):54–59, 2016.

[43] Yael Katz, Kolbjørn Tunstrøm, Christos C Ioannou, Cristián Huepe, and Iain D Couzin. Inferring the structure and dynamics of interactions in schooling fish. *Proceedings of the National Academy of Sciences*, 108(46):18720–18725, 2011.

[44] Chenchen Huang, Feng Ling, and Eva Kanso. Collective phase transitions in confined fish schools. *Proceedings of the National Academy of Sciences*, 121(44):e2406293121, 2024.

[45] VV Isaeva. Self-organization in biological systems. *Biology Bulletin*, 39(2):110–118, 2012.

[46] Giorgio Volpe, Sylvain Gigan, and Giovanni Volpe. Simulation of the active brownian motion of a microswimmer. *American journal of physics*, 82(7):659–664, 2014.

[47] Robert S Cahn, Christopher Ingold, and Vladimir Prelog. Specification of molecular chirality. *Angewandte Chemie International Edition in English*, 5(4):385–415, 1966.

[48] Rustem F Ismagilov, Alexander Schwartz, Ned Bowden, and George M Whitesides. Autonomous movement and self-assembly. *Angewandte Chemie International Edition*, 41(4): 652–654, 2002.

[49] Walter F Paxton, Kevin C Kistler, Christine C Olmeda, Ayusman Sen, Sarah K St. Angelo, Yanyan Cao, Thomas E Mallouk, Paul E Lammert, and Vincent H Crespi. Catalytic nanomotors: autonomous movement of striped nanorods. *Journal of the American Chemical Society*, 126(41):13424–13431, 2004.

[50] Rémi Dreyfus, Jean Baudry, Marcus L Roper, Marc Fermigier, Howard A Stone, and Jérôme Bibette. Microscopic artificial swimmers. *Nature*, 437(7060):862–865, 2005.

[51] Jonathan R Howse, Richard AL Jones, Anthony J Ryan, Tim Gough, Reza Vafabakhsh, and Ramin Golestanian. Self-motile colloidal particles: from directed propulsion to random walk. *Physical review letters*, 99(4):048102, 2007.

[52] Jérémie Palacci, Cécile Cottin-Bizonne, Christophe Ybert, and Lydéric Bocquet. Sedimentation and effective temperature of active colloidal suspensions. *Physical Review Letters*, 105(8):088304, 2010.

[53] Felix Kümmel, Borge Ten Hagen, Raphael Wittkowski, Ivo Buttinoni, Ralf Eichhorn, Giovanni Volpe, Hartmut Löwen, and Clemens Bechinger. Circular motion of asymmetric self-propelling particles. *Physical review letters*, 110(19):198302, 2013.

[54] G Corkidi, B Taboada, CD Wood, A Guerrero, and A Darszon. Tracking sperm in three-dimensions. *Biochemical and biophysical research communications*, 373(1):125–129, 2008.

[55] M Siva Kumar and P Philominathan. The physics of flagellar motion of e. coli during chemotaxis. *Biophysical reviews*, 2(1):13–20, 2010.

[56] Jane Hill, Ozge Kalkanci, Jonathan L McMurry, and Hur Koser. Hydrodynamic surface interactions enable escherichia coli to seek efficient routes to swim upstream. *Physical review letters*, 98(6):068101, 2007.

Curriculum Vitae

Yeray Cruz Ruiz was born in Tlalnepantla, Estado de México, México. He received a Bachelor of Science degree in Mechatronics (2021) from Tecnológico de Monterrey, Campus Monterrey, México, where he is currently a full-time master's student in Nanotechnology, focusing on computational studies of soft matter systems out of thermodynamic equilibrium. His research interests include Soft Matter Physics, Colloidal Models, Spin Systems, Non-Equilibrium Statistical Mechanics, Active Matter, Glassy Systems, and Computational Physics. A passionate advocate for Free and Open Source Software (FOSS), he actively engages in FOSS communities, promoting collaboration and accessibility in scientific research.